Model of stream distribution by sliding wear

Wear, 26 (1973) 105–119

MODEL OF STRAIN DISTRIBUTION BY SLIDING WEAR

J. H. DAUTZENBERG and J. H. ZAAT

Mechanical Engineering Materials Laboratory, University of Technology, Eindhoven (The Netherlands)

(Received February 23, 1973; in final form May 30, 1973)

SUMMARY

On the basis of a model it is possible to describe quantitatively the plastic deformation found in the surface zone of an oxygen free, high conductivity (OFHC) copper pin sliding against an SAE 1045 steel ring.

The proposed model for this deformation type of wear can also be used for all deformation processes actuated by a shear stress on a surface.

NOMENCLATURE

a	distance of an arbitrary point in the material from the sliding surface in μm
A_w	real area of contact in mm^2
b	trackwidth in μm
c	distance from the symmetry plane of the track in μm
$\bar{c}$	average linear intercept of the deformed grain in μm
C	effective stress for $\bar{\delta}=1$ in N/mm^2
$\bar{D}$	average linear intercept of the original grain in μm
F_N	loading force in N
F_W	frictional force in N
l	length of the real area of contact in mm
M	centre of the equishear stress circle
n	work hardening coefficient
P	arbitrary point
R	distance of the point (c, a) from dx in μm
x, y, z	axis of a right hand cartesian coordinate system
x^*, y^*, z^*	along x-axis translated right hand cartesian coordinate system with the centre in M
$\bar{\delta}$	effective strain
d δ_{ij}	incremental natural strains
$\bar{\delta}_S$	effective strain at the surface
$\bar{\delta}_P$	effective strain in point P
ζ	angle of a undeformed grain boundary with the normal of the shear stress plane in rad
θ	angle of a deformed grain boundary with the normal of the shear stress plane in rad

κ geometrical factor
ρ radius of the equishear stress circle in μm
$\bar{\sigma}$ effective stress in N/mm^2
σ_{ij} normal stress components in N/mm^2
$\bar{\sigma}_P$ effective stress in point P
$\bar{\sigma}_S$ effective stress at the sliding surface in N/mm^2
τ_{ij} shear stress components in N/mm^2

1. INTRODUCTION

The sliding couple of an oxygen free, high conductivity (OFHC) copper pin against an SAE 1045 steel ring can under specific conditions and after a short running-in period show exclusively plastic displacement of copper. This flow occurs in the direction of sliding motion and results in an accumulation of material at the trailing edge of the pin (Fig. 1). The accumulated material, the so-called "beard"

Fig. 1. Section of a worn copper pin with "beard". (× 25)

shows a fan-shaped layer structure, typical of this process and is connected with the pin by a thin lip. Displacement of copper occurs only in a very thin surface layer with the maximum thickness close to the "beard". The worn surface of the pin shows a ripple formation (Fig. 2). The surface of the mating ring on the contrary is very smooth with occasional shallow pits originated mainly in the initial stage of the process. This so called *deformation wear process* occurs in the load range 10 to 100 N[1], in an environment ranging from dried air to argon and in mixtures of both and under sliding velocities of 1–5 m/s.

A pin, worn under the above conditions, sectioned perpendicularly to the mating surfaces and to the direction of sliding, exhibits in the vicinity of the

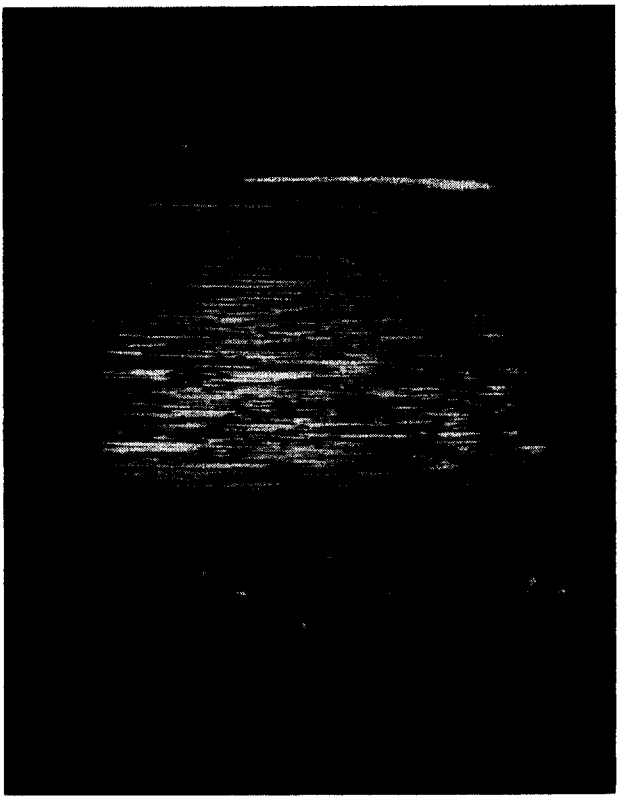

Fig. 2. Worn surface of a copper pin. (× 10)

"beard" deformation fields of a circular shape (Fig. 3). The purpose of this investigation is to describe these fields quantitatively with the help of a model.

The starting point is a stress model which can be transformed into a strain model with the Nadai relation[2]. The strains arrived at in this way can be correlated to the strain found in the sliding couple by means of a linear intercept method published[3] earlier. The derivation of the deformation model and the comparison with the actual deformation will be shown.

2. THE MODEL

In order to describe the effective stress distribution present in the material, one ought to know the forces involved. This will be considered in more detail.

2.1. Determination of the state of stress in the pin at the contact surface

A section, perpendicular to the sliding motion of the pin, (Fig. 3), shows that no transfer of material occurs and that a plain strain[4,5] condition exists. From pin sections in the direction of sliding motion it appears from the unidirectional deflection[3] of the grain boundaries that there is only true shearing. One takes in the real contact surface of extent A_w a right hand cartesian coordinate

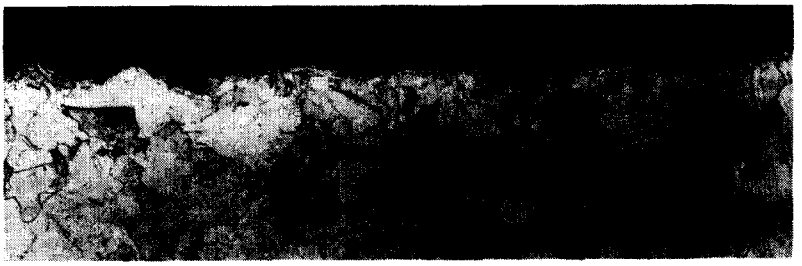

Fig. 3. Deformation fields in a worn copper pin. (× 70)

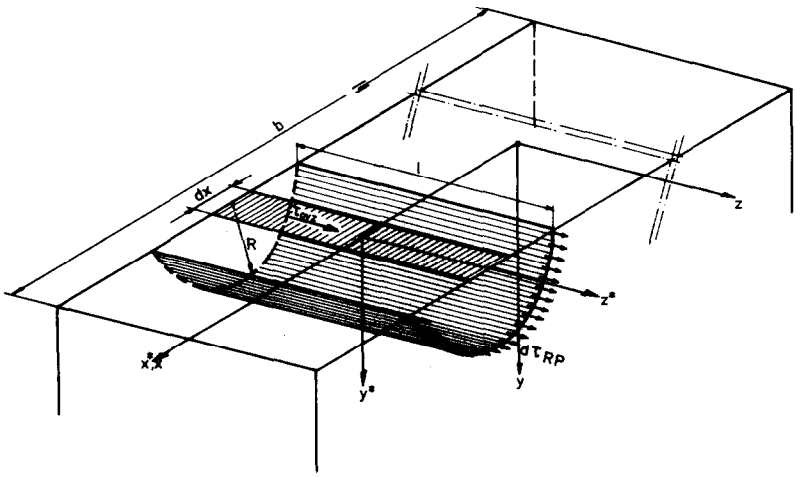

Fig. 4. Equishear stress plane for a track element dx at a distance R.

system so that the y-axis coincides with the direction of the normal force (F_N) and the z-axis coincides with the sliding direction as given in Figs. 4 and 5. The general Levy von Mises equation for a volume element in the contact area with coordinates (x, y, z) and volume $dx\,dy\,dz$ can be written in tensor notation[4,5] as

$$d\delta_y = \frac{3}{2}\frac{d\bar{\delta}}{\bar{\sigma}}\sigma_y$$

or in matrix notation

$$\begin{bmatrix} d\delta_x - d\delta_m & \frac{d\gamma_{yx}}{2} & \frac{d\gamma_{zx}}{2} \\ \frac{d\gamma_{yx}}{2} & d\delta_y - d\delta_m & \frac{d\gamma_{yz}}{2} \\ \frac{d\gamma_{zx}}{2} & \frac{d\gamma_{yz}}{2} & d\delta_z - d\delta_m \end{bmatrix} = \frac{3}{2}\frac{d\bar{\delta}}{\bar{\sigma}} \begin{bmatrix} \sigma_x - \sigma_m & \tau_{yx} & \tau_{zx} \\ \tau_{yx} & \sigma_y - \sigma_m & \tau_{yz} \\ \tau_{zx} & \tau_{yz} & \sigma_z - \sigma_m \end{bmatrix} \quad (2)$$

where $(d\bar{\delta})^2 = \frac{4}{9}\{\frac{1}{2}[(d\delta_x - d\delta_y)^2 + (d\delta_y - d\delta_z)^2 + (d\delta_z - d\delta_x)^2]$

$$+ \tfrac{3}{4}(d\gamma_{yx}^2 + d\gamma_{yz}^2 + d\gamma_{zx}^2)\} \quad (3)$$

$$2\bar{\sigma}^2 = (\sigma_x - \sigma_y)^2 + (\sigma_y - \sigma_z)^2 + (\sigma_z - \sigma_x)^2 + 6\,\tau_{yx}^2 + 6\,\tau_{yz}^2 + 6\,\tau_{zx}^2 = 6k^2 \quad (4)$$

$d\delta_{ij}$ are the incremental natural strain components and $d\sigma_{ij}$ the stress components. Confirming continuity in plastic deformation it holds $d\delta_m = 0$.

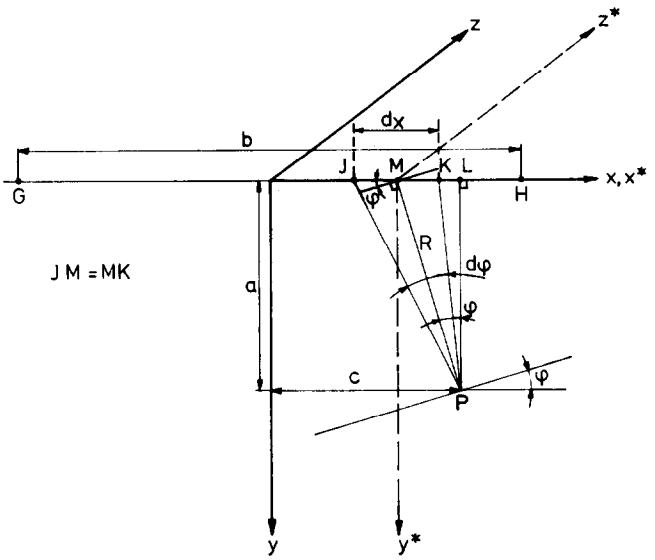

Fig. 5. Shear stress contribution of a track element dx in an arbitrary point P.

In the case of true shearing in the y–z plane

$$d\gamma_{yz} = d\gamma_{zx} = d\delta_x = d\delta_y = d\delta_z = 0 \tag{5}$$

Substituting eqn. (5) in eqn. (2) leads to

$$\begin{bmatrix} 0 & 0 & 0 \\ 0 & 0 & \frac{d\gamma_{yz}}{2} \\ 0 & \frac{d\gamma_{yz}}{2} & 0 \end{bmatrix} = \frac{3}{2}\frac{d\bar{\delta}}{\bar{\sigma}} \begin{bmatrix} \sigma_x - \sigma_m & \tau_{yx} & \tau_{zx} \\ \tau_{yx} & \sigma_y - \sigma_m & \tau_{yz} \\ \tau_{zx} & \tau_{yz} & \sigma_z - \sigma_m \end{bmatrix} \tag{6}$$

From eqn. (6) we conclude that

$$\begin{aligned} &\sigma_x = \sigma_y = \sigma_z = \sigma_m = \tfrac{1}{3}(\sigma_x + \sigma_y + \sigma_z) \\ &\tau_{yx} = 0 \\ &\tau_{zx} = 0 \end{aligned} \tag{7}$$

Substitution in eqn. (4) yields

$$\tau_{yz} = k = \bar{\sigma}/\sqrt{3} \tag{8}$$

This means that the effective stress, causing the effective strain is determined by τ_{yz}, *viz.* the external frictional force (F_W) and not by the load (F_N) normal to the surface.

From eqns. (7) and (4) it can be concluded that the normal force only serves to maintain the hydrostatic pressure and does not influence directly the magnitude of $\bar{\sigma}$.

Considering eqn. (7) and assuming that the contact surface coïncides with the x–z plane, the normal force F_N is given by

$$F_N = \iint_{A_w} \sigma_y(x,z)\,dx\,dz \tag{9}$$

Similarly the frictional force F_W is given by

$$F_W = \iint_{A_w} \tau_{yz}(x,z)\,dx\,dz \tag{10}$$

2.2. Determination of the effective stress distribution in the pin

Consider a real area of contact ($=A_w <$ cross section of the pin) between pin and ring with length l and width b ($l \gg b$) upon which a shear stress τ_{0yz} is operating. Introduce the right hand cartesian coordinate system in such a way that the z-axis bisects b, parallel to l, the x-axis bisects l parallel to b and the y-axis perpendicular to the contact surface A_w. Showing a small part $l\,dx$ of A_w ($dx \ll b$) to which is attached a coordinate system x^*, y^*, z^* originating from the centre of $l\,dx$ and parallel to the x, y and z-axis, the shear stress $d\tau_{RP}$ can be defined as the partial stress due to the shear force acting upon $l\,dx$, working in a half cylindrical surface with the z^* axis as centreline and radius R. (Fig. 4). This results in

$$\tau_{0yz}\,l\,dx = \pi R\,l\,d\tau_{RP} \tag{11}$$

From another section of the track containing the x–y plane (Fig. 5) it will be readily seen that

$$dx = R\,d\phi/\cos\phi \tag{12}$$

Taking into account that

$$d\tau_{RP} = d\tau_{yzP}/\cos\phi \tag{13}$$

where $d\tau_{yzP}$ is the shear stress acting parallel to the x–z plane in P owing to $d\tau_{RP}$.

Equations (11), (12) and (13) result in:

$$\tau_{0yz}\frac{R\,d\phi}{\cos\phi} = \frac{\pi R\,d\tau_{yzP}}{\cos\phi} \tag{14}$$

Sum total of eqn. (14) over the width b gives

$$d\tau_{yzP} = \frac{\tau_{0yz}}{\pi}\int_{\phi_b}^{\phi_l} d\phi \tag{15}$$

where $\phi_b = \text{arctg}\,[(c-\frac{1}{2}b)/a]$ (16)

$\phi_1 = \text{arctg}\,[(c+\frac{1}{2}b)/a]$

Integration and substitution of the limits yields

$$\tau_{yzP} = \frac{\tau_{0yz}}{\pi}\left\{\text{arctg}\left(\frac{c+\frac{1}{2}b}{a}\right) - \text{arctg}\left(\frac{c-\frac{1}{2}b}{a}\right)\right\} \tag{17}$$

or by eqn. (8), eqn. (17) can be written as

$$\bar{\sigma}_P = \frac{\bar{\sigma}_S}{\pi}\left\{\text{arctg}\left(\frac{c+\frac{1}{2}b}{a}\right) - \text{arctg}\left(\frac{c-\frac{1}{2}b}{a}\right)\right\}$$

or

$$\bar{\sigma}_P = \frac{\bar{\sigma}_S}{\pi}\left[\text{arctg}\left\{\frac{a/b}{(a/b)^2+(c/b)^2-1/4}\right\}\right] \tag{18}$$

where $\bar{\sigma}_S$ and $\bar{\sigma}_P$ represent the effective stress in the contact surface and at point P respectively.

3. THE CONSEQUENCE OF THE MODEL USED

To facilitate experimental verification of eqn. (18), this relation for the effective stress is transformed into a relation for effective strain by means of Nadai's law.

For low strain rates and constant temperature this law is given by[2]

$$\bar{\sigma} = C\bar{\delta}^n \tag{19}$$

where C = effective stress by $\bar{\delta} = 1$ (= material constant), n = work hardening coefficient.

Substitution of eqn. (19) in eqn. (18) yields

$$\text{arctg}\left[\frac{a/b}{(a/b)^2+(c/b)^2-1/4}\right] = \pi\frac{\bar{\sigma}_P}{\bar{\sigma}_S} = \pi\left[\frac{\bar{\sigma}_P}{\bar{\delta}_S}\right]^n \tag{20}$$

where $\bar{\delta}_P$ and $\bar{\delta}_S$ equal the effective strain in P and S respectively in the surface, under the assumption that eqn. (19) is valid in the surface. The determination of the effective strain will be dealt with in the appendix. In the following section eqn. (20) will be treated in more detail.

3.1.

Consider a wear track with width b and a constant effective strain $\bar{\delta}_S$ in the surface. In a section perpendicular to this surface and in the direction of sliding eqn. (20) yields for lines of constant strain:

$$\left(\frac{c}{b}\right)^2 + \left(\frac{a}{b} - \frac{1}{2\,\text{tg}\,\kappa}\right)^2 = \left(\frac{1+\text{tg}^2\kappa}{4\,\text{tg}^2\kappa}\right) \tag{21}$$

where by eqn. (20)

$$\kappa = \pi\frac{\bar{\sigma}_P}{\bar{\sigma}_S} = \pi\left(\frac{\bar{\delta}_P}{\bar{\delta}_S}\right)^n = \text{constant} \tag{22}$$

Equation (21) is the equation of a circle with the centre

$$M\left\{0, \frac{b}{2|\text{tg}\kappa|}\right\} \tag{23}$$

and radius

$$\rho = \frac{b}{2|\text{tg}\kappa|}(1+\text{tg}^2\kappa)^{\frac{1}{2}} \tag{24}$$

This circle intersects the x-axis at $\pm b/2$.

From eqns. (20) and (21) it follows that besides the $\bar{\sigma}$–$\bar{\delta}$ relation, given by

the Nadai relation, every increase of $\bar{\sigma}$, which does increase $\bar{\delta}$ monotonous, yields to eqn. (21).

Figures 6, 7 and 8 show computed strain fields for different n but constant $\bar{\delta}_S$.

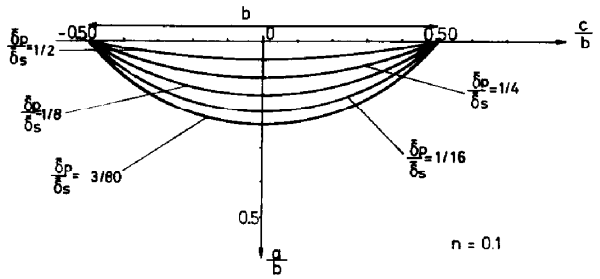

Fig. 6. Equistrain lines for $n=0.1$.

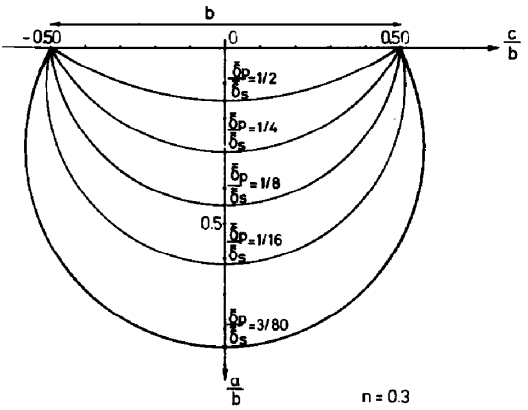

Fig. 7. Equistrain lines for $n=0.3$.

3.2.

Equation (20) can be written as follows

$$\frac{\bar{\delta}_P}{\bar{\delta}_S} = \left[f\left(\frac{a}{b}, \frac{c}{b}\right)\right]^{1/n} \tag{25}$$

$$\text{in which } f\left(\frac{a}{b}, \frac{c}{b}\right) = \frac{1}{\pi} \operatorname{arctg} \left\{ \frac{a/b}{(a/b)^2 + (c/b)^2 - 1/4} \right\} \leqslant 1 \tag{26}$$

For every point of the deformation field holds:

$$\delta_P = f^{1/n} \delta_S \tag{27}$$

With $n < 1$ (physical reality) eqns. (25) and (27) yield the following consequences:

(a) In every point P with the same relative coordinates $(a/b, c/b)$, (f=constant) δ_P/δ_S increases with increasing n. This means that for a constant value of b the relative deformation field δ_P/δ_S penetrates deeper with increasing work hardening coefficient n (Figs. 6, 7 and 8).

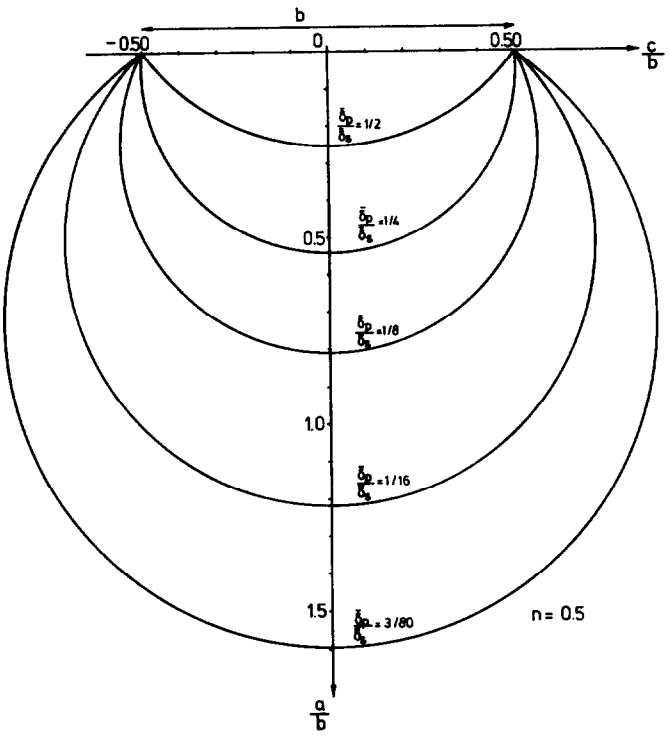

Fig. 8. Equistrain lines for $n=0.5$.

(b) If for a given point P with the relative coordinates (a/b, c/b) n is constant then δ_P/δ_S is constant. This means that the effective strain in point P is proportional to the effective strain δ_S at the surface and that the deformation field penetrates deeper with increasing surface strain δ_S.

(c) Assuming constant values of the work hardening coefficient n and of the effective strain δ_S at the surface it follows that the effective strain δ_P in points having the same relative coordinates a/b and c/b is constant. As a consequence the deformation field will penetrate deeper with increasing track width b and the deformation fields show conformity.

(d) To get information about the maximum depth of the deformation field it is useful to consider the plane of symmetry of the deformation field. For this plane ($c=0$) eqn. (20) yields

$$\left(\frac{a}{b}\right)_{c=0} = \tfrac{1}{2}\,\mathrm{cotg}\left[\frac{\pi}{2}\left(\frac{\delta_P}{\delta_S}\right)^n\right] \tag{28}$$

Defining the maximum depth by a constant value of δ_P it follows when n and δ_S are constant, that the maximum depth is proportional to the trackwidth b. Figure 9 gives a graph of eqn. (28). It follows that the relative maximum depth of the relative deformation field increases with the work hardening coefficient n, as already shown in (a).

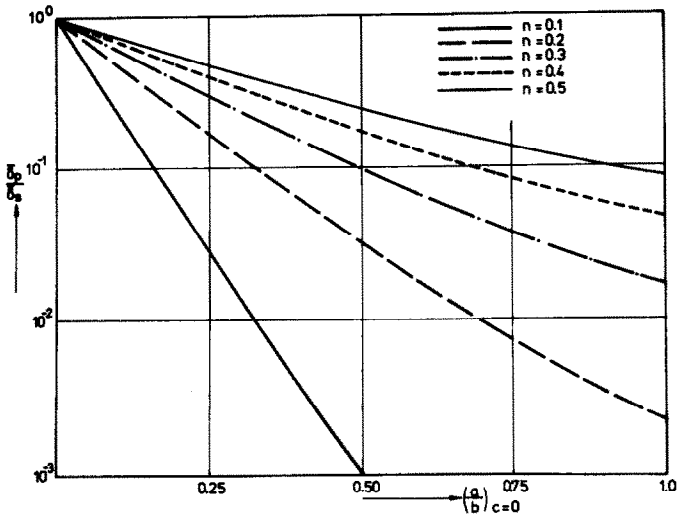

Fig. 9. Strain ratio as a function of $(a/b)_{c=0}$ for different n.

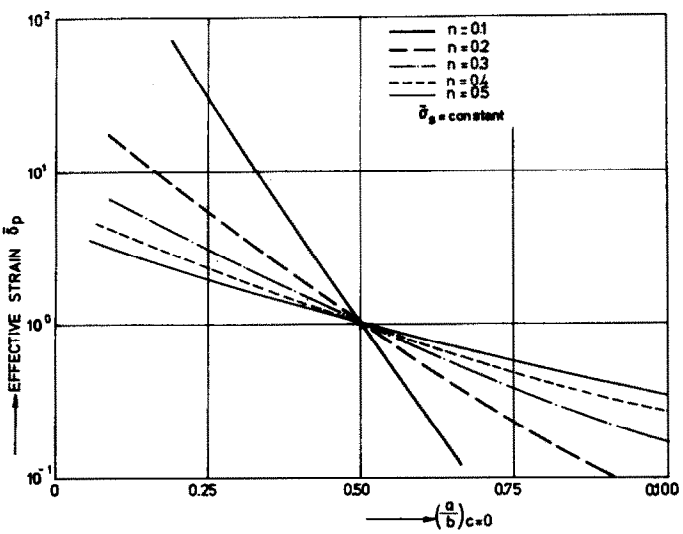

Fig. 10. Effective local strain as a function of $(a/b)_{c=0}$ for different n with $\bar{\sigma}_S = 2\,C$.

(e) Equations (28) and (19) yield:

$$\left(\frac{a}{b}\right)_{c=0} = \tfrac{1}{2}\,\mathrm{cotg}\left[\frac{\pi}{2}\cdot\frac{C\bar{\delta}_P{}^n}{\bar{\sigma}_S}\right] \tag{29}$$

Assuming $\bar{\sigma}_S = \text{constant}$, all curves in the $(a/b)_{c=0}$ *versus* $\bar{\delta}_P$ diagram pass for different values of n through the same point $(\frac{1}{2}\,\mathrm{cotg}\,[\pi C/2\bar{\sigma}],\ 1)$ Figure 10 gives curves for $\bar{\sigma}_S = 2C$ which means $\bar{\delta}_S = 2^{1/n}$ and shows that for increasing n the slope of the $(a/b)_{c=0}$ *versus* $\bar{\delta}_P$ curve will be less negative.

3.3.

From the assumptions in the model it follows that a momentary frictional force F_W and an effective stress $\bar{\sigma}_S$ in the surface of the copper pin, result in a true contact area A_w of

$$A_w = F_W \sqrt{3}/\bar{\sigma}_S \tag{30}$$

3.4.

When for a given track width b, the effective strain $\bar{\delta}_S$ in the contact surface and $\bar{\delta}_P$ in P (c, a) are known, the work hardening coefficient n can be determined by solving eqn. (20) for n. This results in:

$$n = \frac{\log\left[\frac{1}{\pi}\operatorname{arctg}\left\{\frac{a/b}{(a/b)^2+(c/b)^2-1/4}\right\}\right]}{\log\left(\bar{\delta}_P/\bar{\delta}_S\right)} \tag{31}$$

4. PREPARATION OF THE SAMPLES AND EXPERIMENTAL SET-UP

The wear experiments were carried out using a controlled atmosphere pin and ring apparatus with an OFHC copper pin (length 30 mm, diameter 8 mm) and a normalised steel SAE 1045 ring (diameter 82 mm, thickness 10 mm). Test conditions were chosen so that displacement of copper only occurred. The front side of the pin had over a length of 6 mm a quadrangle form with sides of 6 mm. After machining, all copper pins were annealed for three hours at 750°C in vacuum.

Ring and pin were ground and finally polished with 1 μm diamond paste. The pins made macroscopically complete contact with the disk. Sections of the pin for macroscopic investigation were made in the usual manner.

5. EXPERIMENTAL VERIFICATION OF THE MODEL

5.1.

Figures 3 and 11 show the deformation field in the copper pin in a section perpendicular to the contact surface and to the direction of sliding. The circular shape of this deformation field is in agreement with the results obtained from the model (Figs. 6, 7 and 8).

Furthermore it can be seen clearly that different wear tracks overlap. This phenomena has to be taken into account when determining the width b. This width can in good approximation be found by extrapolating the circles to the contact surface of the pin.

5.2.

Plotting the width b of different tracks from the same section—perpendicular to the contact surface and to the sliding direction—with respect to the maximum visible depth $(c=0)$ of the deformation field, the strain is determined by an earlier described method[3] (see also the appendix) and in this case is chosen $\bar{\delta}_P \simeq 1$ (*i.e.* C = constant), a straight line should result according to eqn. (29) if $\bar{\sigma}_S$ = constant.

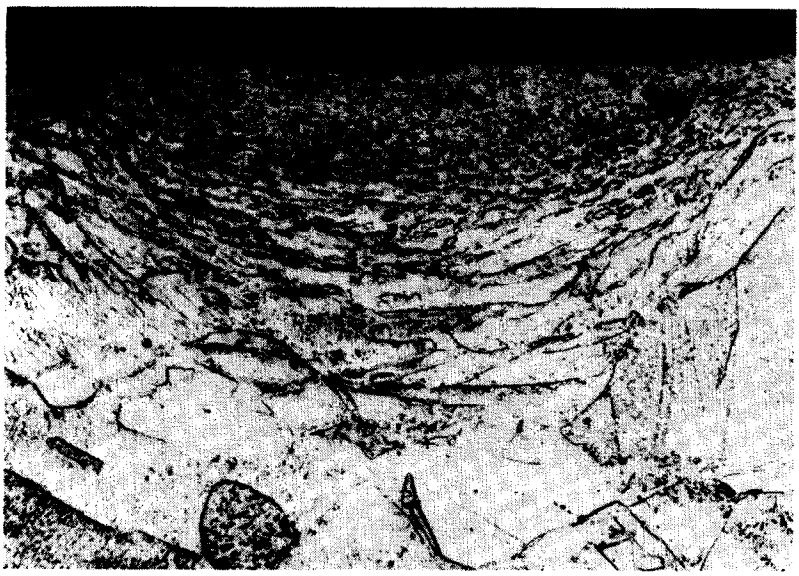

Fig. 11. Deformation field in a worn copper pin. (× 313)

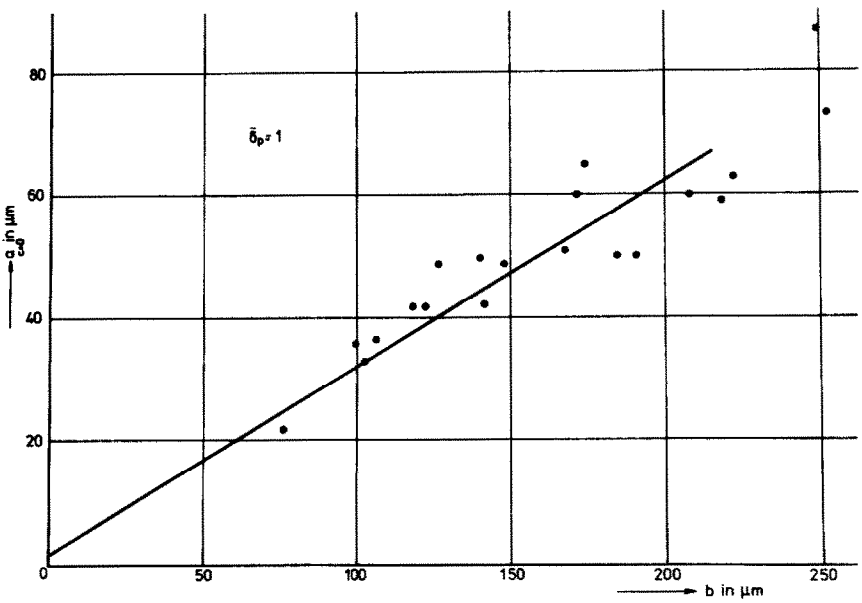

Fig. 12. Experimental relation between strain field penetration and track width.

From experiments (Fig. 12) this line can be found with a correlation coefficient of 0.92 according to the least squares method. This indicates the constancy of $\bar{\sigma}_S$ and the conformity of the deformation fields.

5.3.

The experiments show that the effective strain ($\bar{\delta}_S$), which can be measured[3]

near the surface at a distance of 1–2 mm from the beard, amounts to 20–40. According to Ramaekers[6] the room temperature measured surface microhardness of $H_v = 1600$ N/mm^2 can be transformed into (load 0.25 N) $\bar{\sigma}_S = 560$ N/mm^2. With the aid of $\bar{\sigma}$ and relation (19) it can be deduced that for $C = 400$ N/mm^2 the value of n becomes 0.1. A tensile test at high strain ($\delta > 0.5$) and at room temperature gives a value of $n = 0.18$.

The difference may be due partially to the high strain rate and the high temperature, the latter being at least 100°C higher in the case of this severe wear process as compared with the tensile test. n being 0.1, and the $(a/b)_{c=0}$ ratio from different worn pins from which one is given in Fig. 12, $\bar{\delta}_S$ can be calculated for $\bar{\delta}_P = 1$ according to eqn. (28), ($\bar{\delta}_P$ has been determined experimentally by the method given in the appendix). This results in an average $\bar{\delta}_S$ of 96.

5.4.

Figure 13 gives the experimental results of the effective strain ($= \bar{\delta}_P$) as a function of $(a/b)_{c=0}$ for different track widths.

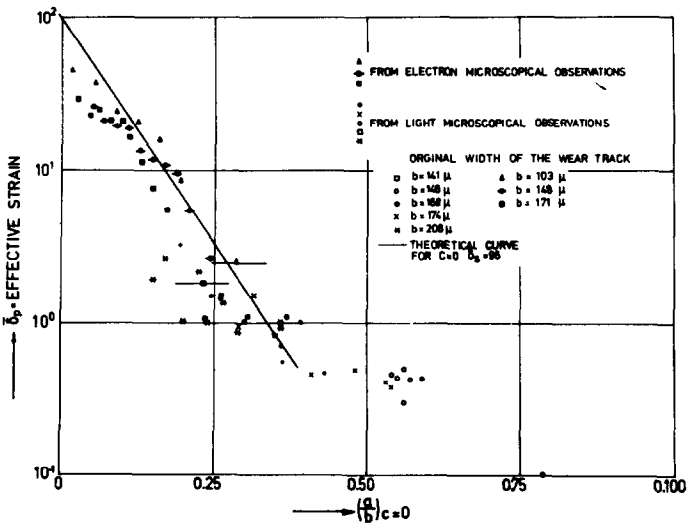

Fig. 13. Interdependence of effective local strain and (a/b).

In this diagram the drawn curve is found with eqn. (28) in which $n = 0.1$, $\bar{\delta}_S = 96$ and $c = 0$. At a short distance ($a/b < 0.1$) from the surface the measured values deviate considerably from the calculated values.
Different causes can be pointed out:

(1) the high strain rate, which is also inhomogeneous, supplied a higher effective stress than that found by the Nadai relation (19)[2].

(2) the relatively high and not equally distributed temperature at the sliding interface. Increased temperature decreases the work hardening coefficient n and the Nadai constancy C[7].

(3) after deformation the copper is less isotropic because of texture and orientation of the crystals. These effects influence the Nadai constants n and C.

In the region where δ_p is small, ($a/b > 0.4$), (Fig. 13), the propagation of strain seems to deviate considerably from the described pattern, resulting in a deeper penetration of the deformation. This can only be explained with an increase of n in that region (Fig. 10). From the tensile test it is known that when δ is low (< 0.5) a high work hardening coefficient is found ($n = 0.5$–0.6).

CONCLUSIONS

(1) Starting with true shearing in the contact surface a model for stress distribution is drafted, from which a description of the deformation field has been derived. The equistrain curves are circles with the track width as a common chord. The position and the radius of the circles are determined by b, n and δ_s.

(2) The proposed model of the deformation fields is in good agreement with the experiments. Besides the nearly exact circular shape of the deformation field a linear relation exists between the depth and the width of these fields for constant δ_s and n.

(3) For large and small strain values in the deformation field the agreement between the model and the experiments deteriorates. This may be due to the changes of the Nadai constants by higher temperature to the high deformation rate, to changes in texture and to recrystallisation which are not taken into account. This requires further elucidation.

(4) The two different work hardening coefficients known from tensile tests are also found when measuring the strain fields of the wear test.

(5) The model gives a method for computing the true contact area.

ACKNOWLEDGEMENTS

The authors are indebted to Messrs. J. A. B. van Dijck and M. J. Links for their experimental assistance.

APPENDIX

The determination of effective deformation under true shearing can be done in two ways *viz.*:

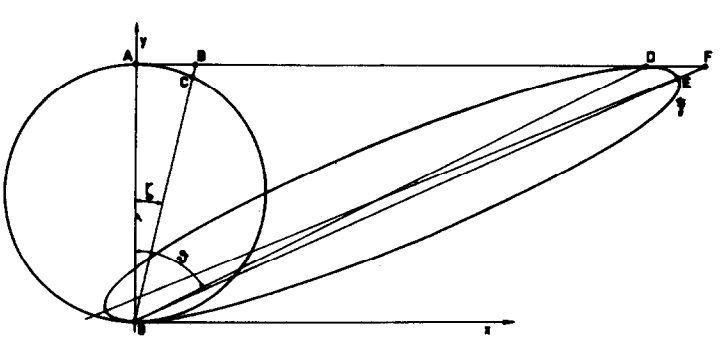

Fig. 14. Deformation of a spherical grain under true shearing.

(1) By means of the deflection of grain boundaries.

(2) By means of the reduction of thickness of metal grains.

Starting from spherical grains subjected to shear stress and looking at a section perpendicular to the interface of the sliding pair and in the sliding direction it can be shown[3], that

$$\delta = (\operatorname{tg}\theta - \operatorname{tg}\zeta)/\sqrt{3} \tag{32}$$

where (Fig. 14) ζ and θ stand for the angle between the grain boundary and the normal on the interface in the unstrained and the strained condition.

Reduction of thickness of metal grains.

It can be shown that

$$\delta = \bar{D}/\bar{c}\sqrt{3} \qquad \bar{D} \gg \bar{c} \tag{33}$$

where $\bar{c}$ and $\bar{D}$ are the mean lengths of the linear intercepts of the respectively strained and unstrained metal grains.

REFERENCES

1 J. H. Dautzenberg and J. H. Zaat, Modell für Gleitverschleiss bei Trockenreibung, *First European Tribology Congress*, London, 1973, paper no. 8 (in press).

2 A. L. Nadai, *Theory of Flow and Fracture of Solids, Vol. 1*, McGraw-Hill, New York, 1950.

3 J. H. Dautzenberg and J. H. Zaat, Quantitative determination of deformation by sliding wear, *Wear*, 23 (1973) 9–19.

4 P. C. Veenstra, *Grondslagen van de Mechanische Technologie*, Technische Plasticiteitsleer, Technische Hogeschool, Eindhoven.

5 E. G. Thomsen, C. T. Yang and S. Kobayashi, *Mechanics of Plastic Deformation in Metal Processing*, Macmillan Co., New York, 1965.

6 J. A. H. Ramaekers, *Härte und Verformung Metallischer Werkstoffe Dokterarbeit*, Technische Hogeschool, Eindhoven.

7 H. G. Grewe und E. Kappler, Über die Ermittlung der Verfestigungskurve durch den Torsionsversuch an zylindrischen Vollstäben und das Verhalten von vielkristallinem Kupfer bei sehr hoher plastischer Schubverformung, *Phys. status solidi*, 6 (1964) 339.